



LIBRARY
ROYAL AIRCRAFT ESTABLISHMENT
BEDFORD.

MINISTRY OF TECHNOLOGY
AERONAUTICAL RESEARCH COUNCIL
CURRENT PAPERS

The Distribution of a Wall Pressure Rise
in a Turbulent Boundary Layer

By

R.J. Herd

LONDON: HER MAJESTY'S STATIONERY OFFICE

1967

Price 6s. 6d. net

C.P. No. 967

November, 1965

The Distribution of a Wall Pressure Rise
in a Turbulent Boundary Layer*

- By -
R.J. Herd

SUMMARY

An expression is derived for the wall pressure gradient in attached flow with both compressible and incompressible turbulent boundary layers. From this gradient, the pressure distribution may be determined by an integration process, and it is seen that the agreement with experiment is encouraging. Of the various potential applications of this technique, separation is here considered.

*Replaces N.G.T.E. R.275 - A.R.C.27 733

CONTENTS

- 1. Introduction
- 2. Determination of the Pressure Distribution
 - 2.1 Theory
 - 2.2 Practice
- 3. Prediction of Separation
- 4. Possible Future Work
- 5. Conclusions

Acknowledgement

References

Distribution

Detachable Abstract Cards

APPENDICES

<u>No.</u>	<u>Title</u>
I	Notation
II	Definitions
III	Compressible Flow

ILLUSTRATIONS

<u>Fig. No.</u>	<u>Title</u>
1	Incompressible Separation Flow Model
2	Basic Curve - I
3	Basic Curve - II
4	Comparison with Experiment
5	Effect of Shape Parameter
6	Effect of Reynolds number
7	Effect of Length
8	Effect of Length and Reynolds number
9	Mach number 1.5 Results
10	Separation Prediction Methods
11	Mach number 2 Results

1. Introduction

In a variety of aerodynamic problems, a knowledge of the boundary layer wall pressure distribution is of interest. This wall pressure distribution governs the rate of thickening of the boundary layer, and conversely the rate of thickening of the boundary layer governs the pressure distribution along its free-stream edge. Consequently the details of the flow are determined by the equilibrium of these two effects.

Many formulae have been evolved which claim to compute the growth of incompressible boundary layers. By the use of such a formula, it will be shown how an expression for the wall pressure gradient may be derived for compressible flow with the aid of a transformation technique. Turbulent behaviour is covered in some detail, and the same general approach may be used for laminar flow. On equating this pressure gradient with that of the free-stream at the edge of the boundary layer, the expression may be numerically integrated to give the variation of pressure with streamwise distance.

Such a technique has a number of relevant applications in various fields of aerodynamics. In this paper, its application to the prediction of separation is considered.

2. Determination of the Pressure Distribution

An expression is derived in Appendix III for the wall pressure gradient in attached flow with a compressible turbulent boundary layer.

2.1 Theory

In any application of the analysis to boundary layer problems where the pressure distribution is required, a relation is necessary between an angle ϕ (as in Fig. 1) and the free-stream flow conditions. It is assumed in this instance that the effect of the boundary layer on the free-stream flow is equivalent to a displacement of the wall surface by an amount equal to the displacement thickness of the boundary layer. Some theoretical justification for this statement is given in Ref. 1.

The required relation for supersonic flow is simply obtained. As is well known, the thickening of the boundary layer leads to the emergence of an infinite number of compression waves from the free-stream surface. These eventually coalesce to form the familiar oblique shock wave. Clearly there is a loss of total pressure through this shock, but this loss is much reduced near the boundary layer surface by the "cushioning effect" of the boundary layer itself. It is therefore plausible to assume that the flow near the edge of the boundary layer is locally isentropic, and so to employ the familiar Prandtl-Meyer equation in order to relate the angle of the flow to its Mach number.

The Prandtl-Meyer equation with supersonic flow enables the pressure gradient at any point to be calculated. By a simple process of numerical integration, the whole distribution can be determined since

$$P = P_1 + \int_{x_1}^x \frac{dP}{dx} \cdot dx \quad \dots(1)$$

In/

In the turbulent case, calculation of the incipient boundary layer functions must entail an allowance for any initial region of laminar flow.

Before moving to the numerical integration process itself, it is perhaps worthwhile to consider some of the assumptions involved in this technique.

(i) Two-dimensional flow

As it stands, the analysis is only true for two-dimensional flow.

(ii) Nature of the free-stream flow

Compressible flow is assumed, and it is taken to be isentropic, with $\gamma = 1.40$.

(iii) Boundary layer assumptions

The usual assumptions are made, and although generally valid, their accuracy diminishes in steep pressure gradients.

(iv) Boundary layer relations

In this paper, the following relations have been employed:

- (a) Maskell for incompressible momentum thickness.
- (b) Maskell for incompressible shape parameter behaviour.
- (c) Ludwig and Tillman for skin friction.
- (d) Power law relation for viscosity.
- (e) Stratford and Beavers for compressible momentum thickness.

All are of sufficient standing to justify confidence in their use, but as with most boundary layer solutions, one tends to be wary of their accuracy near separation or reattachment.

(v) Free-stream flow direction

It has been assumed here that the equivalent boundary of the inviscid flow is obtained by displacing the wall surface by an amount equal to the displacement thickness of the boundary layer.

(vi) Free-stream behaviour

The Prandtl-Meyer equation is used in conjunction with an assumption of incompressible flow near the boundary layer surface. It is conceivable that a better approximation to the truth may be made by taking the compression at the boundary layer edge to occur through a series of small shocks, instead of through a Prandtl-Meyer turn.

(vii) Transform

Mager's modification of the Stewartson transform has been used, largely because of the ease with which the various parameters of interest can be

transformed/.

transformed. Nevertheless, a certain amount of justifiable suspicion is inevitably attracted to work involving transforms of the turbulent boundary layer, and only a successful comparison between theory and experiment can wholly justify such an approach.

The numerical integrations were carried out on a digital computer.

2.2 Practice

The first problem to arise concerned the initial data. Unless otherwise stated, it is taken throughout this analysis that the flow is two-dimensional and supersonic. Up to the incipient point there is no pressure gradient, and the boundary layer is always fully turbulent. At the incipient point itself, it is assumed that the boundary layer velocity profile is given by a power law.

Six further variables are now required to define completely the incipient conditions. These are the stagnation pressure $\{P_t\}$ and temperature $\{T_t\}$, and the incipient Mach number (M_1) , x co-ordinate (x_1) , shape parameter (H_1) and boundary layer slope (ϕ_1) . In fact, were random values given to these quantities, the flow model would be fully defined, and the incipient

value of $\left(\frac{dM}{dx}\right)$ could be calculated. However, we know that $\left(\frac{dM}{dx}\right)$ at the incipient point is zero, and one of the six parameters is therefore redundant.

Unfortunately, were the calculation started with $\left(\frac{dM}{dx}\right)$ equal to zero, the exponential nature of the pressure rise would ensure that separation occurred only at infinity. This is clearly ridiculous, and the problem was overcome

by selecting a value for the term $\left(\frac{dM}{dx}\right)_1$, and using this as an incipient point condition. From the limited quantity of accurate experimental data

available, it was found that when $\left(\frac{dM}{dx}\right)_1$ is put equal to $-\frac{1}{9}$, reasonable

agreement with experiment occurs. This value was used throughout, and the angle ϕ_1 omitted from the set of initial conditions. It should be pointed out

that the only effect of a change in $\left(\frac{dM}{dx}\right)_1$ is upon the scale in the x direction of the foot of the distribution; the gradient and pressure rise of the steep portion, and the pressure rise of the foot remain constant.

Having defined the initial conditions the question of step length arose. Various lengths were employed, and eventually it was found that the best compromise of speed and accuracy was such that the change in Mach number at each step was equal to 0.1% of the incipient Mach number (M_1) .

It is now possible to consider an example of the method. Stagnation conditions of 2 atm and 300°K were arbitrarily chosen, as were the incipient Mach number of 2, x co-ordinate of 1 ft, and velocity profile power law exponent of 5. These lead to an incipient flat plate Reynolds number of 7.3 million. Fig. 2 gives the resultant pressure distribution. Although the

initial part of the pressure curve is sensible, the method indicates that it becomes horizontal as separation is approached, and this portion of the curve is omitted from Fig. 2. Experience leads one to believe that this inaccuracy near separation might occur, and there appear to be three contributory factors. First, the failure of the familiar Prandtl assumptions in steep pressure gradients. Second, the inaccuracy of the expression for C_f nearing separation. And finally the Maskell relations, which become suspect as separation is approached. If the technique is to be of any use at all, this problem must be overcome.

In this instance there is a means of evading the trouble. Reference to separation pressure distributions, such as those of Chapman et al², demonstrates that beyond the initial foot of the distribution, $\left(\frac{dP}{dx}\right)$ is effectively constant up to separation. It is therefore possible to obtain a more realistic pressure curve merely by extrapolating the predicted curve from its point of inflection. The modified curve is given in Fig. 3. It should be pointed out that the scale of plotting the curve differs from that normally used for experimental separation data, the ultimate pressure gradient here appearing to be much less steep.

Adequate curves of the pressure rise associated with turbulent flat plate separation are rare. This is especially true of the initial foot of the rise, and even in the data of Chapman et al² here used, the shape is far from certain. For the same incipient conditions, a comparison between theory and experiment is given in Fig. 4. It can be seen from Fig. 5 that the dependence of the theoretical curve upon the incipient value of n is critical, and unfortunately this is the one condition which cannot be simply determined. With a seventh power law profile, the agreement is poor, with a fifth, good.

It is possible to determine n_1 by first calculating $Re_{\theta,1}^*$ from Eqn. (A89). Maskell³ presents a relation between H^* and Re_{θ}^* for flow on a flat plate with zero pressure gradient such as occurs at the incipient point. From H_1^* one can obtain H_1 by Eqn. (A90), whence n_1 is found. If this procedure is adopted for the incipient flow relevant to Fig. 4, n_1 is found to be equal to 5.0.

One can now proceed to examine the effects of several variables. Keeping the stagnation temperature at 300°K and the incipient Mach number at 2, it is possible to vary the stagnation pressure and incipient x co-ordinate. In turn, changes in these quantities affect the incipient flat plate Reynolds number.

Keeping all except stagnation pressure and hence flat plate Reynolds number the same, the effect of alterations in these two quantities is shown in Fig. 6.

Turning to the question of length, Fig. 7 demonstrates the results of modifications to the incipient x co-ordinate whilst maintaining constant the flat plate Reynolds number by adjusting the stagnation pressure. It is interesting that the gradient of the steep slope is no different, the whole effect being similar to that caused by a shift in $\left(\frac{dM}{dx}\right)_1$. When plotted on an absolute length scale, a sizeable difference is to be seen.

A similar treatment, but now changing merely the value of x and not the stagnation pressure, is given in Fig. 8.

So far, work has been confined to Mach number 2. In order to complete the picture, examples of the method were carried out at other conditions, bearing in mind that the flow must never become subsonic. A case at Mach number 1.5 is presented in Fig. 9, demonstrating a noticeable change in the steepest gradient when compared with Mach number 2 results.

At Mach number 2.5 sensible curves were obtained, but near 3 the method failed. Since the technique as a whole appears to be sound, one must conclude that the values of A, B, C and D are incorrect. One immediately suspects the transform, and other work, notably on base pressure problems, seems to confirm this suspicion.

3. Prediction of Separation

Having examined the present method as a means of determining the distribution of a pressure rise in a compressible turbulent boundary layer, one can now turn to the prediction of separation. Several incompressible techniques exist to calculate the point of separation, and it should therefore be possible to adapt these to compressible flow by means of a transformation. All require a prior knowledge of the pressure distribution, and this is now available. Of the incompressible treatments, five of the more important will be considered, namely those due to Buri⁴, Maskell³, Spence⁵, Stratford⁶, and Truckenbrodt⁴. A paper by Smith⁷ considers them in detail.

(i) Buri

Buri⁴ derives an expression for the change with distance of his own boundary layer parameter, and claims that separation occurs when this parameter reaches a chosen value.

(ii) Maskell

Using his equations³ for the rate of change of shape parameter, the local skin friction coefficient may be determined. Since this coefficient is inaccurately determined near separation, it is necessary to extrapolate the curve to zero, at which point separation takes place.

(iii) Spence

Having presented equations similar to Maskell, but in a simplified form, Spence⁵ proposes that separation occurs when the shape parameter is between 2 and 3.

(iv) Stratford

Stratford⁶ demonstrates that there is an equation relating several variables which is only true when the skin friction has fallen to zero - e.g., at separation.

(v) Truckenbrodt

In a manner comparable to that of Maskell³ and Spence⁵, Truckenbrodt⁴ derives an expression from which the shape parameter can be found. He then proposes that separation takes place when the shape parameter lies between 1.8 and 2.4.

Time and space prevent a detailed consideration of all five methods. Maskell's relations for the rate of change of shape parameter have already been used. For the determination of separation, the skin friction technique of Maskell and the critical shape parameter concepts of Spence and Truckenbrodt will be employed.

Taking first the skin friction extrapolation, Fig. 10 shows the basic pressure distribution, together with curves of skin friction and shape parameter. As can be seen, the skin friction method greatly overestimates the separation pressure rise. That this is no isolated example is indicated by Figs. 3 to 9. An improvement might follow the use of a direct compressible skin friction equation, but such a development is probably not worthwhile, since the inherent error in the use of a skin friction technique makes it less attractive than the shape parameter method.

Passing to the critical shape parameter, experiment suggests that separation occurs when the incompressible shape parameter is 2.14 (see Fig. 10). This is almost mid-way between the limits proposed by Truckenbrodt⁴, and is also contained by those of Spence⁵. It thus seems plausible to take the mean of the values quoted by Truckenbrodt as giving the separation point (i.e., $H^* = 2.1$). For $M = 2$, Figs. 3 to 10 show this to be reasonably accurate for an initial compressible power law profile exponent of 5, but it becomes progressively less accurate as the exponent increases (i.e., H_1^* decreases). This leads us to the conclusion that some account must be taken of the incipient shape parameter, and the use of a constant ratio of separation to incipient incompressible shape parameter is one such possibility. With this ratio equal to 1.541, Figs. 9 and 11 demonstrate that there is indeed an improvement, but further refinement is precluded by the lack of evidence as to the precise effect of n_1 upon the separation pressure rise.

4. Possible Future Work

The previous sections describe a method of predicting the distribution of a pressure rise in a turbulent boundary layer with compressible flow. There seem to be four main routes along which future development could possibly proceed.

In first place there is the extension of the technique to deal with laminar flow. This should present no great difficulty.

Then there is the application to separation, as discussed in Section 3. Besides improving the means of predicting separation, factors such as the effect of wall shape on the pressure rise to separation might be examined. In the light of Reference 8, knowledge of the effect of longitudinal wall curvature would be of especial interest.

Thirdly, by considering various types of solid surface geometry, the distribution of pressure over several flow models might be determined. As an instance, the unseparated pressure distribution of flow over aerofoils or cylinders could be calculated.

Finally, several aspects of reattachment behaviour could be investigated. Since the skin friction at reattachment is zero - as at separation - the relation between the reattachment pressure and the eventual downstream pressure might be derived in much the same way that the separation work was carried out.

5. Conclusions

An expression has been derived for the wall pressure gradient in attached flow with a compressible turbulent boundary layer. From this gradient, the pressure distribution may be determined by an integration process, and the agreement with experiment is encouraging. Of the various potential applications of this technique, separation has been here considered.

Acknowledgement

The author wishes to acknowledge the important part played by Mr. J.B. Roberts in first formulating this treatment.

References/

References

<u>No.</u>	<u>Author(s)</u>	<u>Title, etc.</u>
1	A.D. Young	The calculation of the profile drag of aerofoils and bodies of revolution at supersonic speeds. A.R.C.15 970, April, 1953.
2	D.R. Chapman, D.M. Kuehn and H.K. Larson	Investigation of separated flows in supersonic and subsonic streams with emphasis on the effect of transition. N.A.C.A. Report 1356, 1958.
3	E.C. Maskell	Approximate calculation of the turbulent boundary layer in two-dimensional incompressible flow. R.A.E. Report No. Aero 2443, November, 1961. A.R.C.14 654.
4	H. Schlichting	Boundary layer theory. McGraw-Hill Book Co. Inc., New York, 1955.
5	D.A. Spence	Aerofoil theory - the flow in turbulent boundary layers. A.R.C.18 261, March, 1956.
6	B.S. Stratford	The prediction of separation of the turbulent boundary layer. Journal of Fluid Mechanics, Vol. 5, Part I, 1959.
7	D.J.L. Smith	Turbulent boundary layer theory and its application to blade profile design. N.G.T.E. Memorandum No. M.395, March, 1965. A.R.C. C.P.868.
8	M.V. Herbert and R.J. Herd	Boundary layer separation in supersonic propelling nozzles. A.R.C. R. & M. 3421, August, 1964.
9	V.A. Sandborn	Preliminary experimental investigation of low-speed turbulent boundary layers in adverse pressure gradients. N.A.C.A. T.N.3031, October, 1953.
10	H. Ludwig and W. Tillmann	Investigation of the wall shearing stresses in turbulent boundary layers. N.A.C.A. T.M.1285, May, 1950.
11	B.S. Stratford	Flow in the laminar boundary layer near separation. A.R.C. R. & M. 3002, November, 1954.
12	B.S. Stratford and G.S. Beavers	The calculation of the compressible turbulent boundary layer in an arbitrary pressure gradient - a correlation of certain previous methods. A.R.C. R. & M.3207, September, 1959.
13	A. Mager	Transformation of the compressible turbulent boundary layer. J. Aero. Sci., Vol. 25, No. 5, p.305, May, 1958.

APPENDIX I

Notation

A	$\frac{\partial \theta}{\partial x}$
B	$\frac{\partial \theta}{\partial M_e}$
C	$\frac{\partial H}{\partial x}$
C_f	local skin friction coefficient
D	$\frac{\partial H}{\partial M_e}$
F	transform function
G	transform function
g	gravitational acceleration
H	boundary layer shape parameter $\left(\frac{\delta^*}{\theta} \right)$
M, M_e	Mach number at boundary layer free-stream edge
n	velocity profile power law exponent
P	pressure (static unless with suffix t)
P'	$M_e^4 (1 + 0.2 M_e^2)^{-4}$
Re	Reynolds number per unit length
Re_X	Reynolds number based upon X
Re_θ	Reynolds number based upon θ
R_G	gas constant

T temperature (static unless with suffix t)

U free-stream velocity

W $\frac{1}{Re} \cdot \frac{dRe}{dM_e}$

X equivalent flat plate length

x Cartesian co-ordinate

Y Maskell function

Z Maskell function

Γ Maskell function

γ ratio of specific heats

δ* boundary layer displacement thickness

θ boundary layer momentum thickness

$\bar{\theta}$ $\theta Re_{\theta}^{0.2155}$

μ viscosity

ρ density

Φ Maskell function

φ $\tan^{-1} \left(\frac{d\delta^*}{dx} \right)$

ω viscosity - temperature relation exponent

Suffices

e boundary layer free-stream edge

T turbulent

t total head

i incipient

* transformed - i.e., incompressible (except δ*)

∞ undisturbed free-stream.

APPENDIX II

Definitions

Equivalent flat plate length	X	That length over which a boundary layer growing on a flat plate at the local Mach number would attain the same thickness as the actual boundary layer
Flat plate Reynolds number	Re_X	$\left(\frac{\rho_e U_e}{\mu_e} \right) \cdot X$ where the density, velocity and viscosity are those at the free-stream edge
Momentum Reynolds number	Re_θ	$\left(\frac{\rho_e U_e}{\mu_e} \right) \cdot \theta$ where the density, velocity and viscosity are those at the free-stream edge

Incipient pressure	P_1	Pressure at the incipient point, just ahead of the separation pressure rise
Separation pressure	P_s	Pressure at the separation point

APPENDIX III

Compressible Flow

General Expression for Pressure Gradient

By definition $\delta^* = H \cdot \theta \quad \dots(A1)$

whence $d\delta^* = H \cdot d\theta + \theta \cdot dH \quad \dots(A2)$

By definition $\frac{d\delta^*}{dx} = \tan \phi \quad \dots(A3)$

i.e., $d\delta^* = dx \tan \phi \quad \dots(A4)$

It will be shown later that the increments $d\theta$ and dH may be expressed as

$$d\theta = \frac{\partial \theta}{\partial x} \cdot dx + \frac{\partial \theta}{\partial M_e} \cdot dM_e \quad \dots(A5)$$

and $dH = \frac{\partial H}{\partial x} \cdot dx + \frac{\partial H}{\partial M_e} \cdot dM_e \quad \dots(A6)$

Let $A = \frac{\partial \theta}{\partial x}$

$$B = \frac{\partial \theta}{\partial M_e}$$

$$C = \frac{\partial H}{\partial x}$$

$$D = \frac{\partial H}{\partial M_e} \quad \dots(A7)$$

Then Eqns. (A2) to (A7) give

$$dx \tan \phi = H(A dx + B dM_e) + \theta(C dx + D dM_e) \quad \dots(A8)$$

which, /

which, when rearranged and taken to its limits, yields

$$\frac{dM_e}{dx} = \left[\frac{\tan \phi - HA - \theta C}{HB + \theta D} \right] \quad \dots(A9)$$

For $\gamma = 1.40$,

$$\frac{P_t}{P} = (1 + 0.2 M_e^2)^{\frac{7}{2}} \quad \dots(A10)$$

Assuming P_t to remain constant

$$\frac{dP}{dM_e} = - \left[\frac{1.4 M_e P}{1 + 0.2 M_e^2} \right] \quad \dots(A11)$$

whence

$$\frac{dP}{dx} = - \frac{1.4 M_e P}{1 + 0.2 M_e^2} \cdot \frac{\tan \phi - HA - \theta C}{HB + \theta D} \quad \dots(A12)$$

The various terms

It is suggested in Ref. 12 that for free-stream flat plate Reynolds numbers of the order of 10^6 , the momentum thickness of a turbulent boundary layer can be expressed as

$$\theta = 0.036 (1 + 0.1 M_e^2)^{-0.7} X Re_X^{\frac{1}{5}} \quad \dots(A13)$$

this expression being valid in an arbitrary pressure gradient, where

$$X = \frac{1}{P'} \int_0^x P' dx \quad \dots(A14)$$

and

$$P' = \left[\frac{M_e}{1 + 0.2 M_e^2} \right]^4 \quad \dots(A15)$$

It is to be understood that these last three equations are only valid for air with $\gamma = 1.40$.

Rewriting/

Rewriting Eqn. (A13)

$$\theta = 0.036 (1 + 0.1 M_e^2)^{-0.7} X^{\frac{4}{5}} Re^{-\frac{1}{5}} \quad \dots(A16)$$

$$\therefore \frac{1}{\theta} d\theta = - \frac{0.14 M_e}{1 + 0.1 M_e^2} dM_e + \frac{4}{5X} dX - \frac{1}{5Re} dRe \quad \dots(A17)$$

Eqn. (A14) gives

$$\frac{1}{X} dX = \frac{1}{X} dx - \frac{1}{P'} dP' \quad \dots(A18)$$

and Eqn. (A15) gives

$$\frac{1}{P'} dP' = \frac{4 (1 - 0.2 M_e^2)}{M_e (1 + 0.2 M_e^2)} dM_e \quad \dots(A19)$$

By definition

$$Re = \frac{\rho_e U_e}{\mu_e} \quad \dots(A20)$$

$$U_e = (\gamma_g R_G T_t)^{\frac{1}{2}} M_e (1 + 0.2 M_e^2)^{-\frac{1}{2}} \quad \dots(A21)$$

$$\rho_e = \rho_t (1 + 0.2 M_e^2)^{-\frac{5}{2}} \quad \dots(A22)$$

and
$$\left(\frac{\mu_e}{\mu_t} \right) = \left(\frac{T_e}{T_t} \right)^\omega \quad \dots(A23)$$

$$\therefore Re = \frac{\rho_t}{\mu_t} (\gamma_g R_G T_t)^{\frac{1}{2}} M_e (1 + 0.2 M_e^2)^{\omega - \frac{3}{2}} \quad \dots(A24)$$

$$\therefore W = \frac{1}{Re} \cdot \frac{dRe}{dM_e} = \frac{1 + (0.4 \omega - 1) M_e^2}{M_e (1 + 0.2 M_e^2)} \quad \dots(A25)$$

Combining/

Combining Eqns. (A17) to (A19) and Eqn. (A25) yields

$$A = \frac{4\theta}{5X} = 0.01255 (1 + 0.1 M_e^2)^{\frac{7}{8}} Re_{\theta}^{-\frac{1}{4}} \quad \dots(A26)$$

$$B = -\theta \left[\frac{0.14 M_e}{(1 + 0.1 M_e^2)} + \frac{3.2 (1 - 0.2 M_e^2)}{M_e (1 + 0.2 M_e^2)} + \frac{W}{5} \right] \quad \dots(A27)$$

For free-stream flat plate Reynolds numbers near 10^7 , Stratford and Beavers¹² quote

$$\theta = 0.022 (1 + 0.1 M_e^2)^{-0.7} X Re_X^{-\frac{1}{8}} \quad \dots(A28)$$

In this case analysis as above gives

$$A = \frac{5\theta}{6X} = 0.00855 (1 + 0.1 M_e^2)^{-0.84} Re_{\theta}^{-\frac{1}{8}} \quad \dots(A29)$$

$$B = -\theta \left[\frac{0.14 M_e}{(1 + 0.1 M_e^2)} + \frac{3.33(1 - 0.2 M_e^2)}{M_e (1 + 0.2 M_e^2)} + \frac{W}{6} \right] \quad \dots(A30)$$

An alternative means of deriving A and B involves the use of a suitable transform. Here, the Mager¹³ modification of the Stewartson transform is used. This employs two functions:

$$F = \left(\frac{T_e}{T_t} \right)^{\frac{1}{2}} \quad \dots(A31)$$

$$G = \left(\frac{\mu_e}{\mu_t} \right) F^{\frac{2}{\gamma-1}} \quad \dots(A32)$$

Now it is a condition of the transform that when the pressure across the boundary layer perpendicular to the wall is assumed to be constant

$$\frac{\mu_t}{\mu_e}$$

$$\frac{\mu_t}{\mu_e} = \frac{T_t}{T_e} \quad \dots(A33)$$

although Eqn. (A23) is a more accurate form of this relation. For $\gamma = 1.4$

$$F = (1 + 0.2 M_e^2)^{\frac{1}{2}} \quad \dots(A34)$$

$$G = (1 + 0.2 M_e^2)^{-\frac{7}{2}} = F^7 \quad \dots(A35)$$

Now, by definition

$$\theta = \bar{\theta} \frac{1}{1.2155} \text{Re} \frac{0.2155}{1.2155} \quad \dots(A36)$$

$$\therefore d\theta = \frac{\theta}{1.2155\bar{\theta}} d\bar{\theta} - \frac{0.2155\theta}{1.2155 \text{Re}} d\text{Re} \quad \dots(A37)$$

But $\frac{d\text{Re}}{dM_e} = W \text{Re}$

$$\therefore d\theta = \frac{\theta}{1.2155\bar{\theta}} d\bar{\theta} - \frac{0.2155W\theta}{1.2155} dM_e \quad \dots(A38)$$

The transform yields three relations:

$$\bar{\theta}^* = F^{6.431} \bar{\theta} \quad \dots(A39)$$

$$dx^* = F^6 dx \quad \dots(A40)$$

$$U_e^* = F^{-1} U_e \quad \dots(A41)$$

On differentiation

$$\frac{1}{\bar{\theta}^*} d\bar{\theta}^* = \frac{6.431}{F} dF + \frac{1}{\bar{\theta}} d\bar{\theta} \quad \dots(A42)$$

and/

and
$$dF = -0.2 M_e F^3 dM_e \quad \dots(A43)$$

Thus
$$d\theta = \frac{F^{-6.431} \theta}{1.2155 \bar{\theta}} d\bar{\theta}^* + \frac{1.2862 M_e F^2 \theta}{1.2155} dM_e - \frac{0.2155 W \theta}{1.2155} dM_e \dots(A44)$$

Further¹
$$d\bar{\theta}^* = 0.01173 dx^* - 4.200 \frac{\bar{\theta}^*}{U_e^*} dU_e^* \quad \dots(A45)$$

and
$$dU_e^* = -F^{-2} U_e dF + F^{-1} dU_e \quad \dots(A46)$$

or
$$dU_e^* = U_e F^{-1} M_e^{-1} dM_e \quad \dots(A47)$$

whence
$$d\bar{\theta}^* = 0.01173 F^6 dx - 4.200 \bar{\theta} F^{6.431} M_e^{-1} dM_e \quad \dots(A48)$$

Combining Eqns. (A44) and (A48) gives

$$A = 0.00965 (1 + 0.2 M_e^2)^{-0.7645} Re_\theta^{-0.2155} \quad \dots(A49)$$

$$B = -\theta \left[\frac{3.4554}{M_e} - \frac{1.0582 M_e}{1 + 0.2 M_e^2} + 0.1773 W \right] \quad \dots(A50)$$

Eqns. (A49) and (A50) are in close numerical agreement with Eqns. (A26) and (A29), and (A27) and (A30) respectively.

C and D are also derived by transforming Maskell's³ incompressible relations.

$$\frac{dH^*}{dx^*} = \theta^{*-1} Re_\theta^{*-0.266} \Phi(\Gamma^*, H^*) \quad \dots(A51)$$

where
$$\Gamma^* = \frac{0.246}{C_f^*} \cdot \frac{\theta^*}{U_e^*} \cdot \frac{dU_e^*}{dx^*} \quad \dots(A52)$$

and¹⁰
$$C_f^* = 0.246 e^{-1.561H^*} Re_\theta^*^{-0.268} \dots(A53)$$

$\phi(\Gamma^*, H^*)$ is shown³ to be capable of expression as

$$\phi(\Gamma^*, H^*) = Y + Z\Gamma^* \dots(A54)$$

with Y and Z functions of H^* alone, although the functions themselves change according to the magnitude of Γ^* . Thus

$$dH^* = \theta^{*-1} Re_\theta^*^{-0.268} Y dx^* + e^{1.561H^*} U_e^*{}^{-1} Z dU_e^* \dots(A55)$$

As before $dx^* = F^\theta dx \dots(A56)$

and $U_e^* = F^{-1} U_e \dots(A57)$

It can be shown that

$$\theta^* = F^\theta \theta \dots(A58)$$

$$Re_\theta^* = F^2 Re_\theta \dots(A59)$$

$$H = H^* (1 + 0.2 M_e^2) + 0.2 M_e^2 \dots(A60)$$

Thus
$$dH^* = \theta^{-1} Re_\theta^{-0.268} Y F^{1.464} dx + e^{1.561H^*} Z M_e^{-1} dM_e \dots(A61)$$

But, on differentiating Eqn. (A60)

$$dH = (1 + 0.2 M_e^2) dH^* + 0.4 M_e (1 + H^*) dM_e \dots(A62)$$

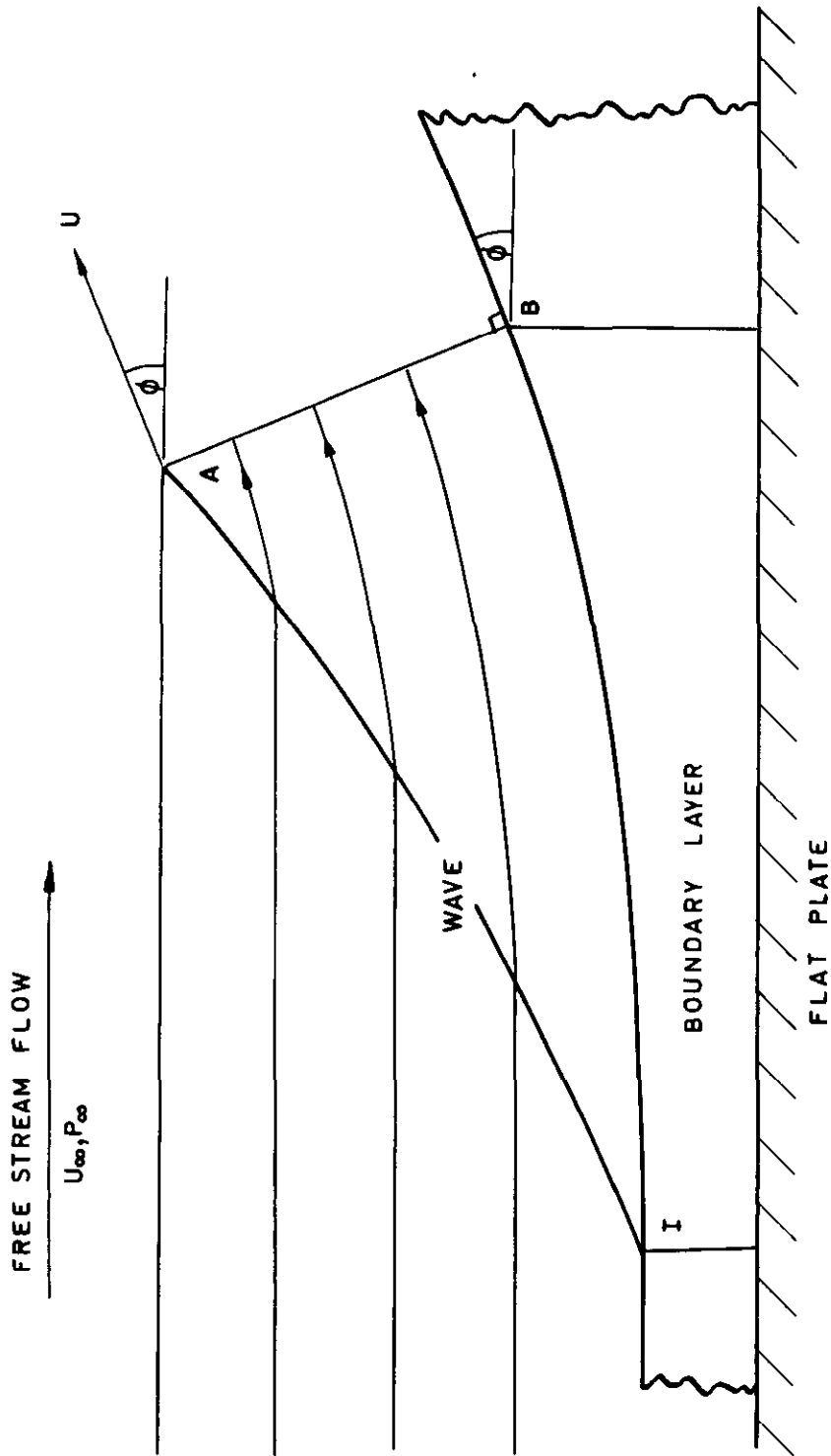
whence it is clear, from Eqns. (A61) and (A62), that

$$C = (1 + 0.2 M_e^2)^{0.268} \theta^{-1} Re_\theta^{-0.268} Y \quad \dots(A63)$$

$$D = 0.4 M_e (1 + H^*) + (1 + 0.2 M_e^2) M_e^{-1} \theta^{1.561} H^* Z \quad \dots(A64)$$

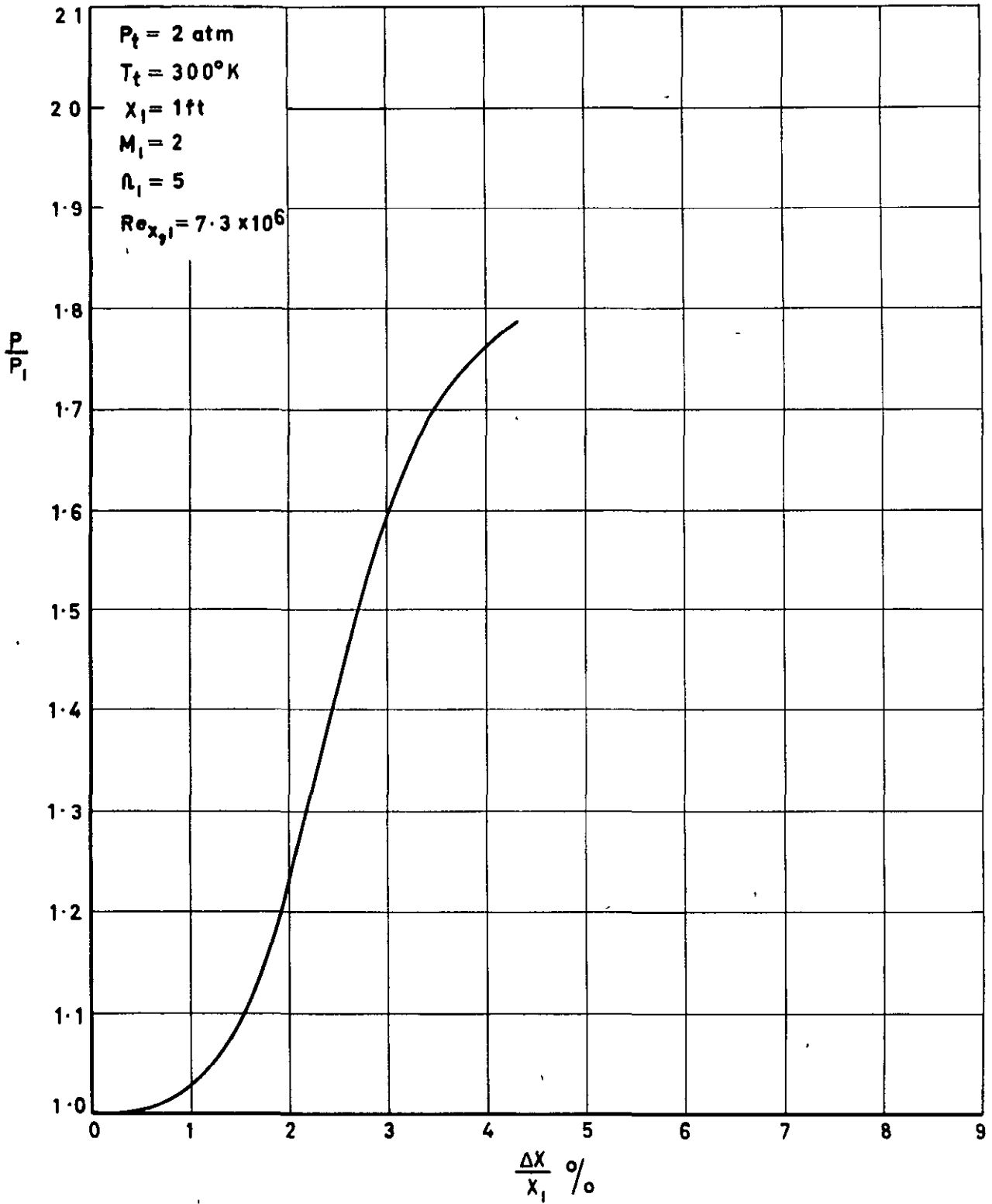
As with incompressible flow, the technique may also be applied to laminar boundary layers by replacing the appropriate turbulent equations by their laminar counterparts.

FIG. 1



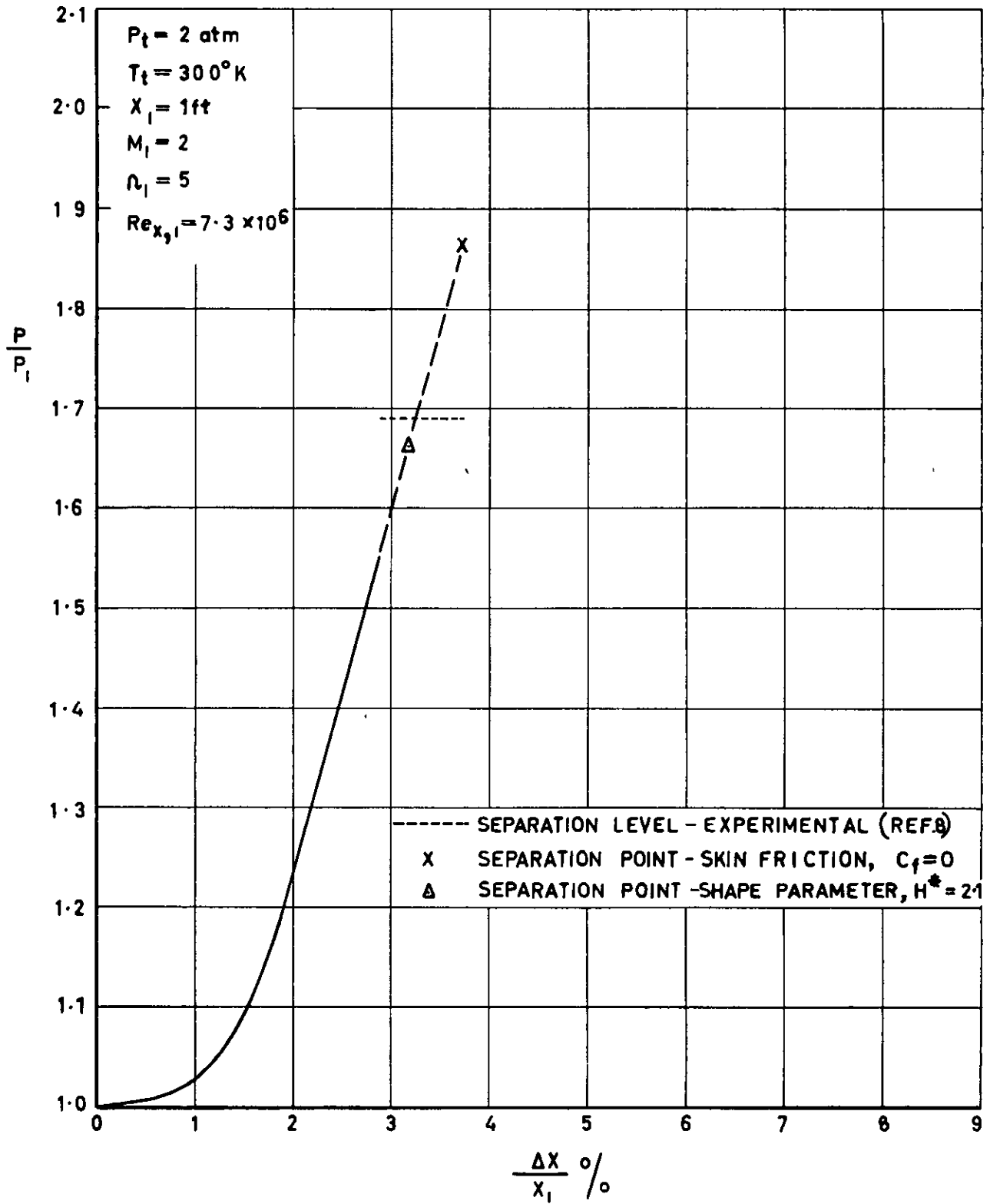
INCOMPRESSIBLE SEPARATION FLOW MODEL.

FIG. 2



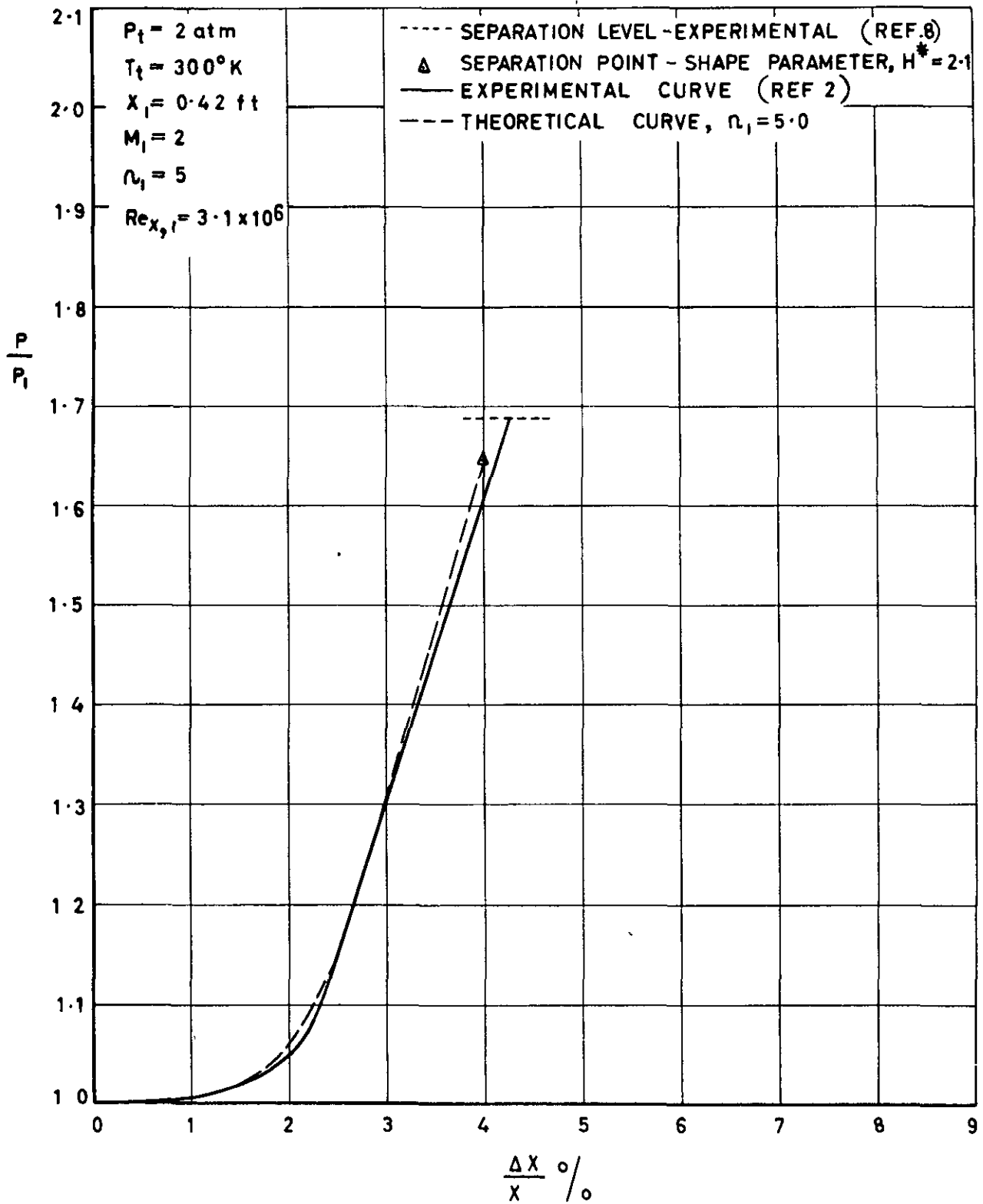
BASIC CURVE - I.

FIG. 3



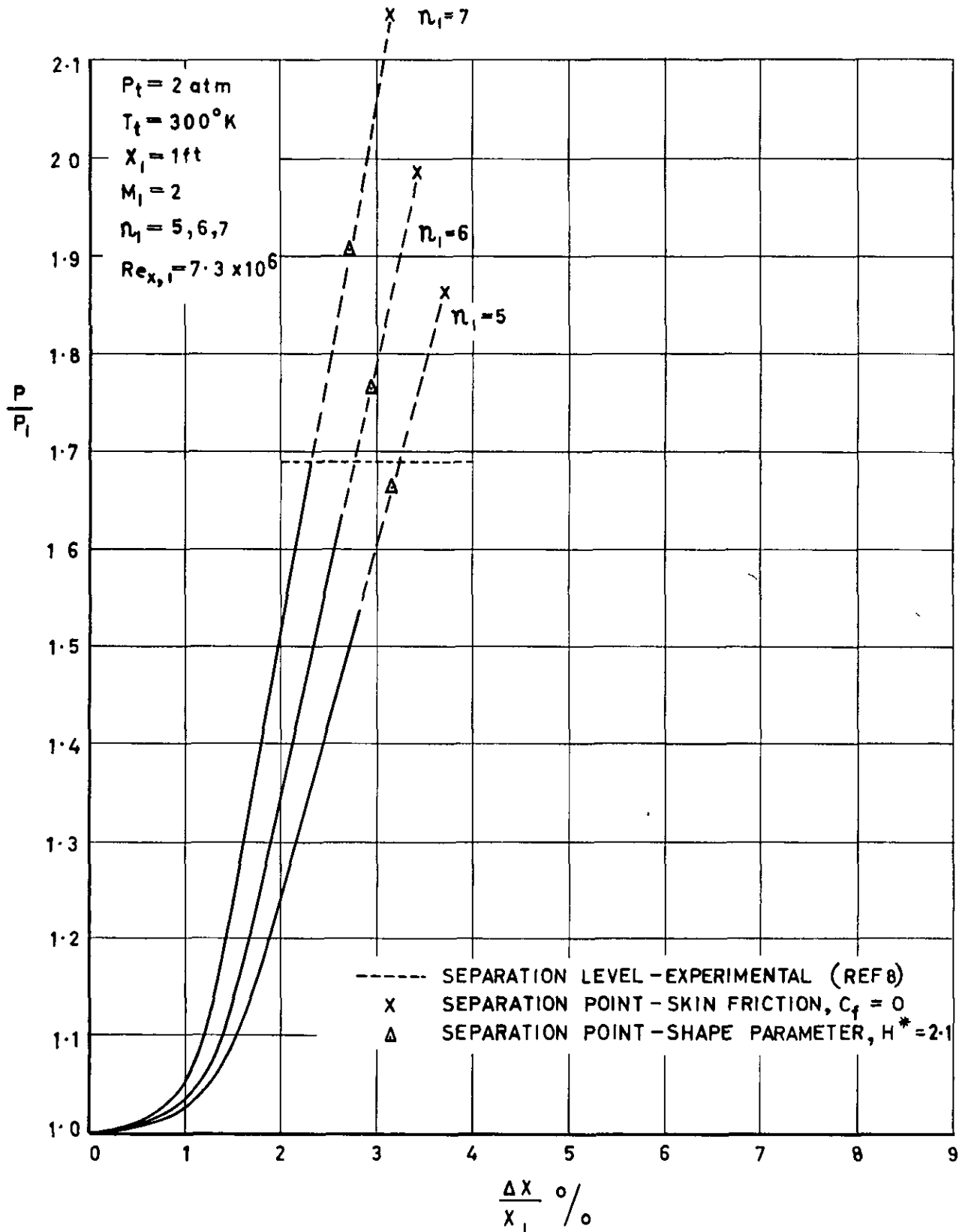
BASIC CURVE - II.

FIG. 4



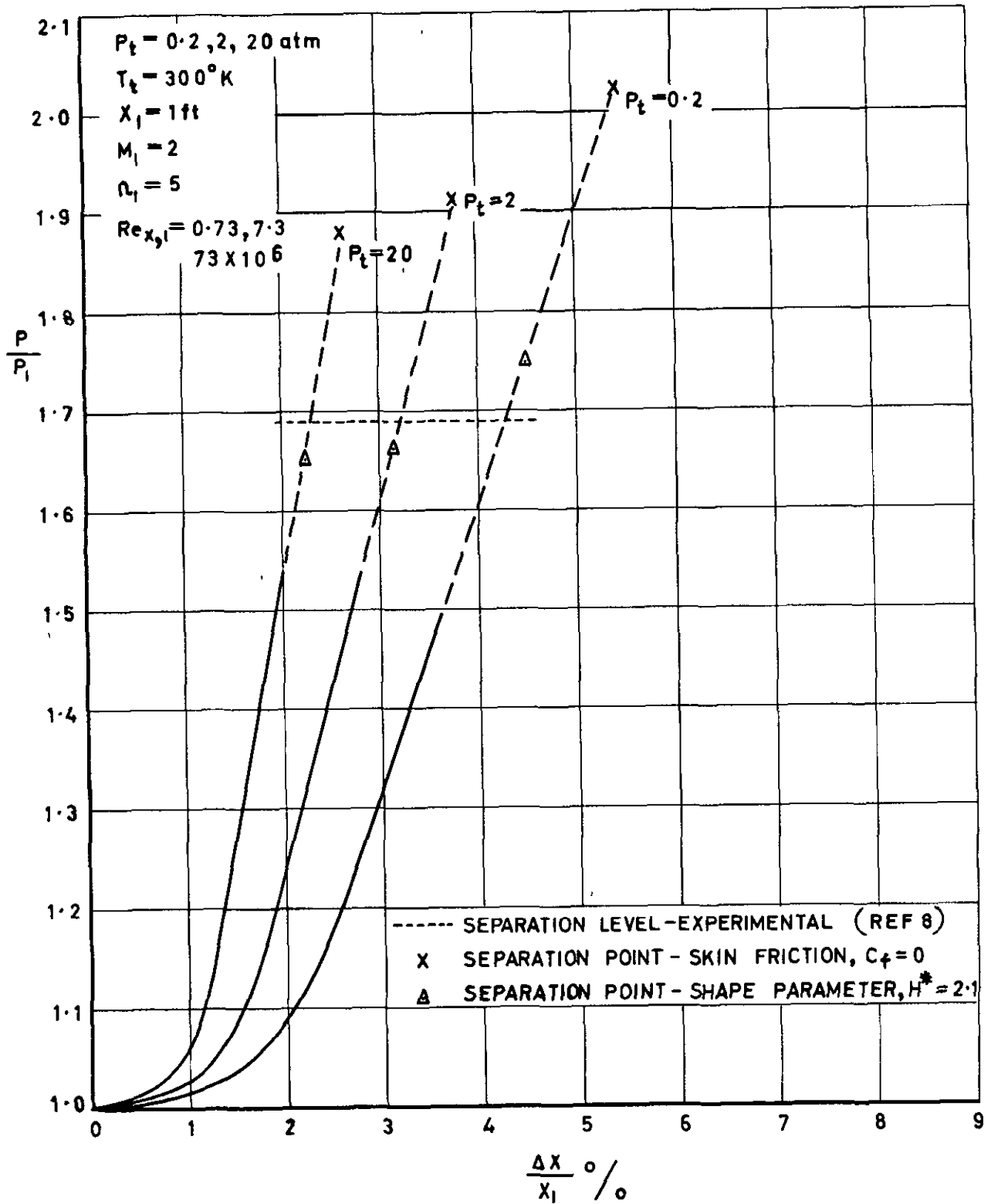
COMPARISON WITH EXPERIMENT.

FIG. 5



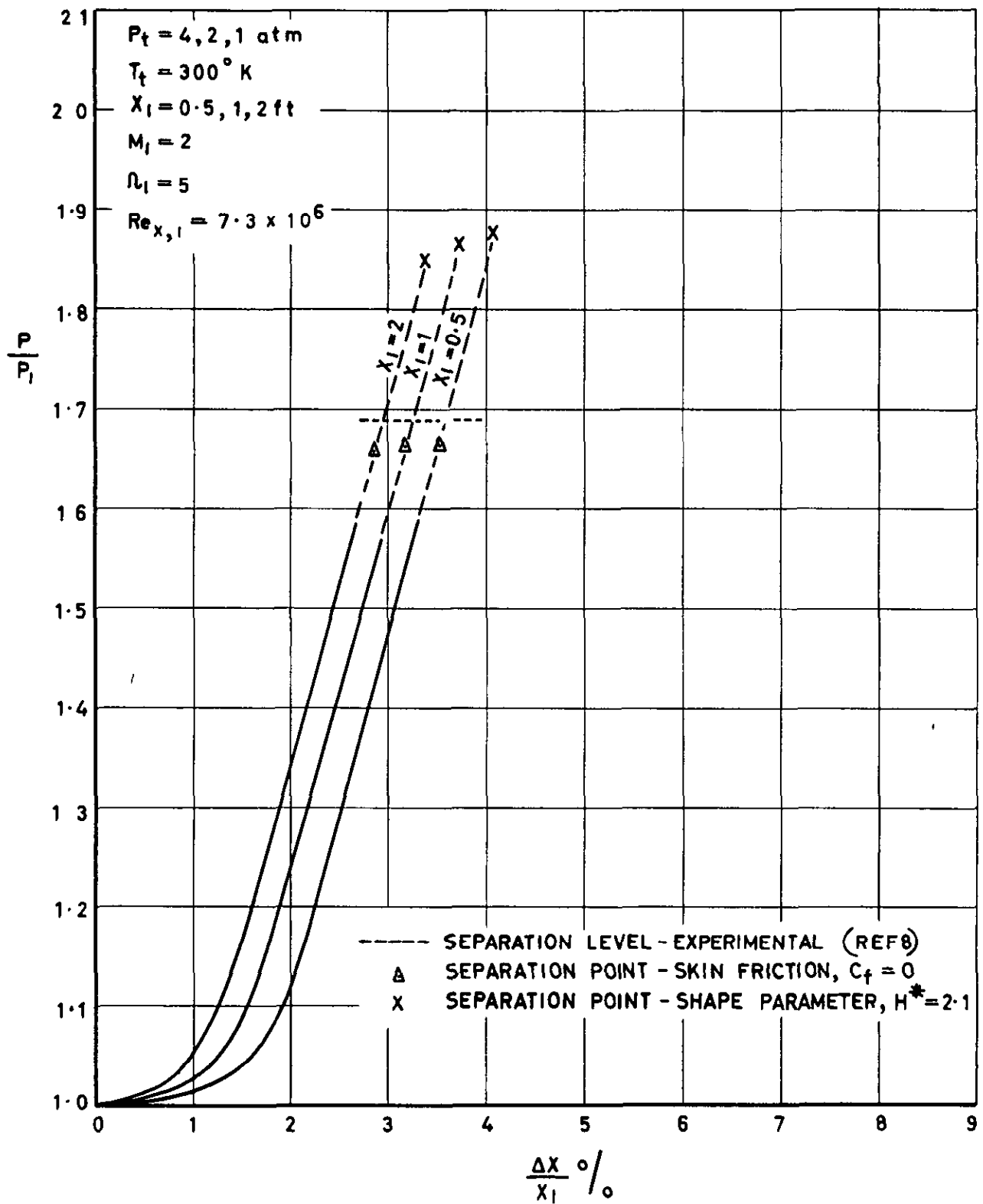
EFFECT OF SHAPE PARAMETER.

FIG. 6



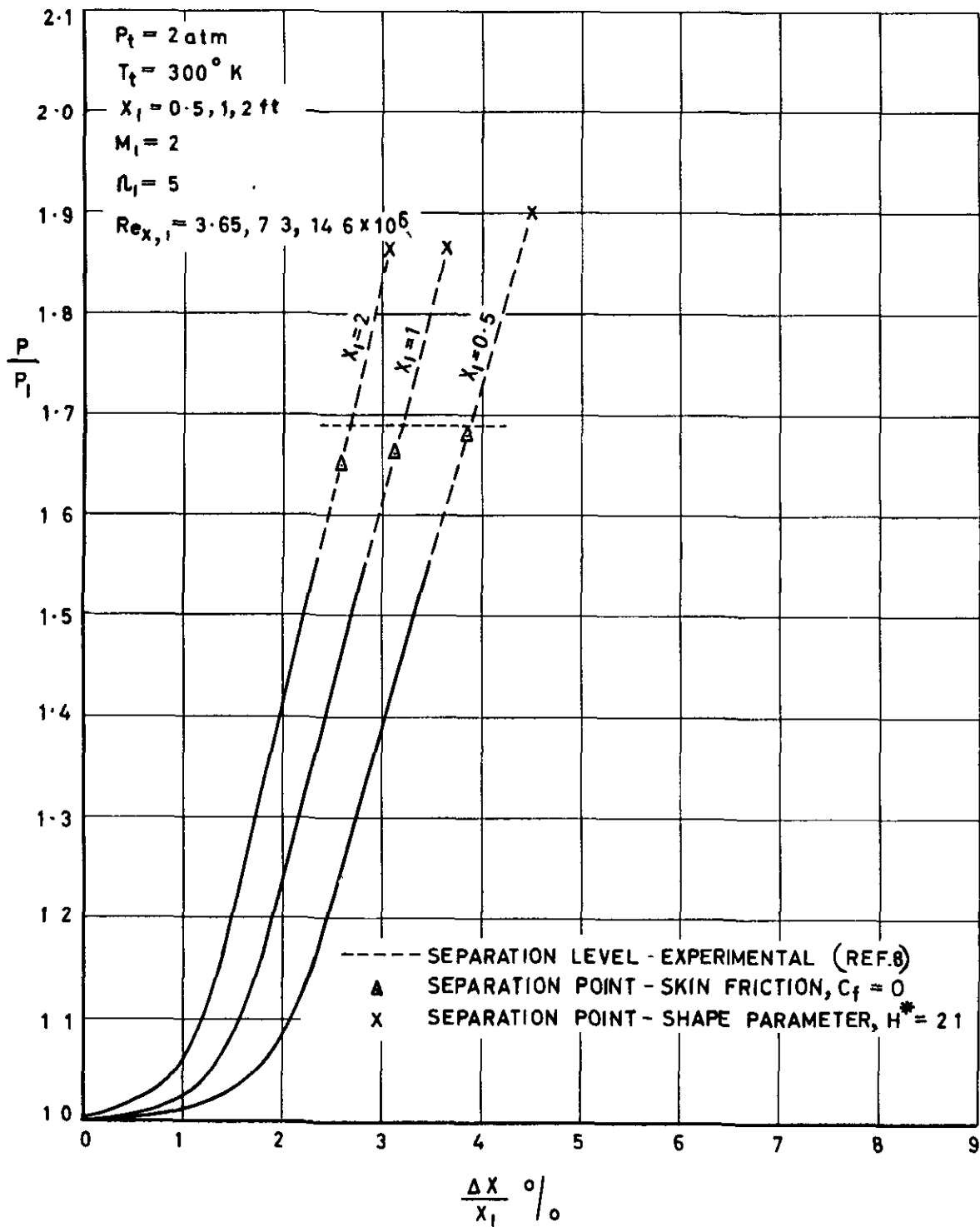
EFFECT OF REYNOLDS NUMBER.

FIG. 7



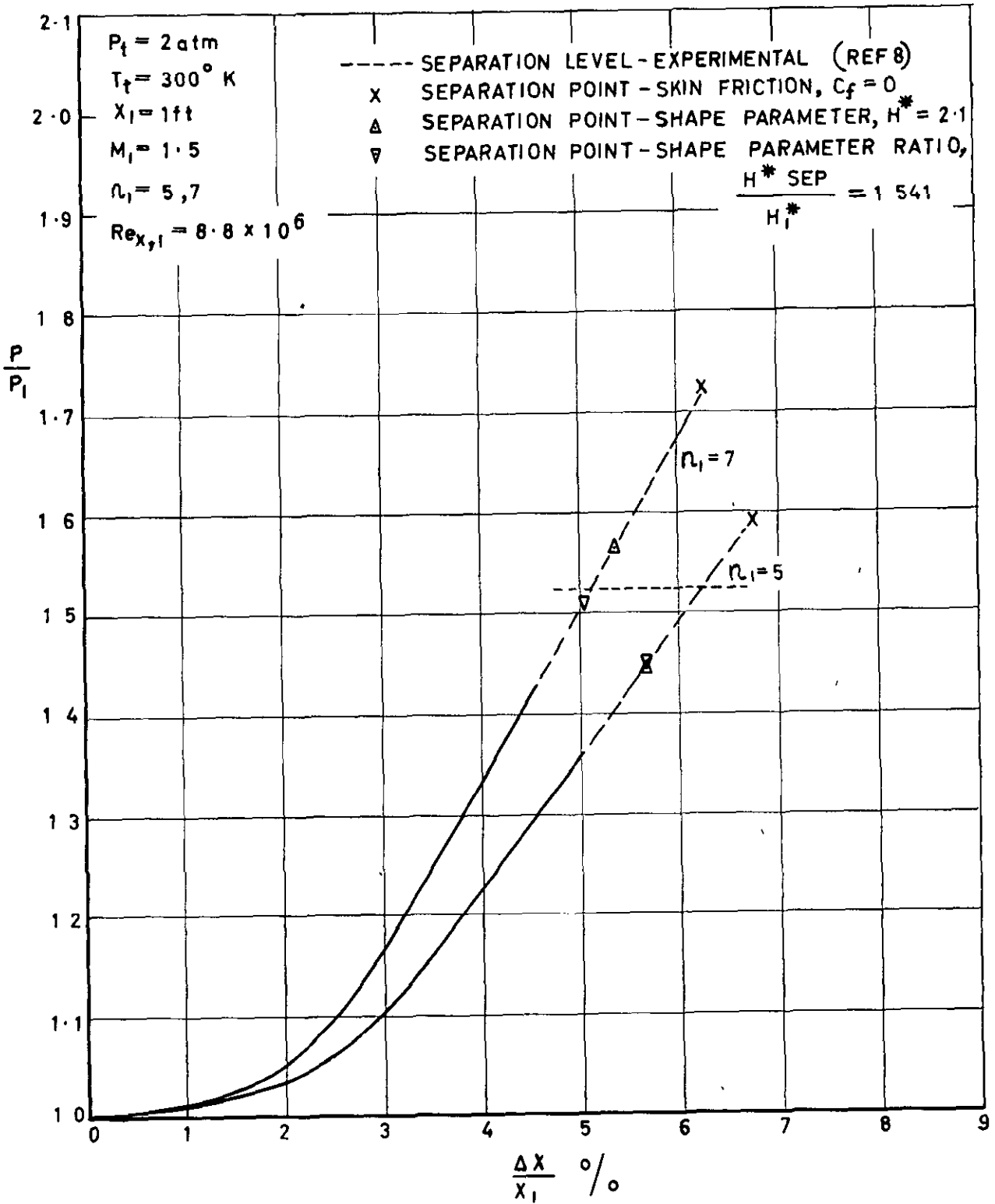
EFFECT OF LENGTH.

FIG. 8



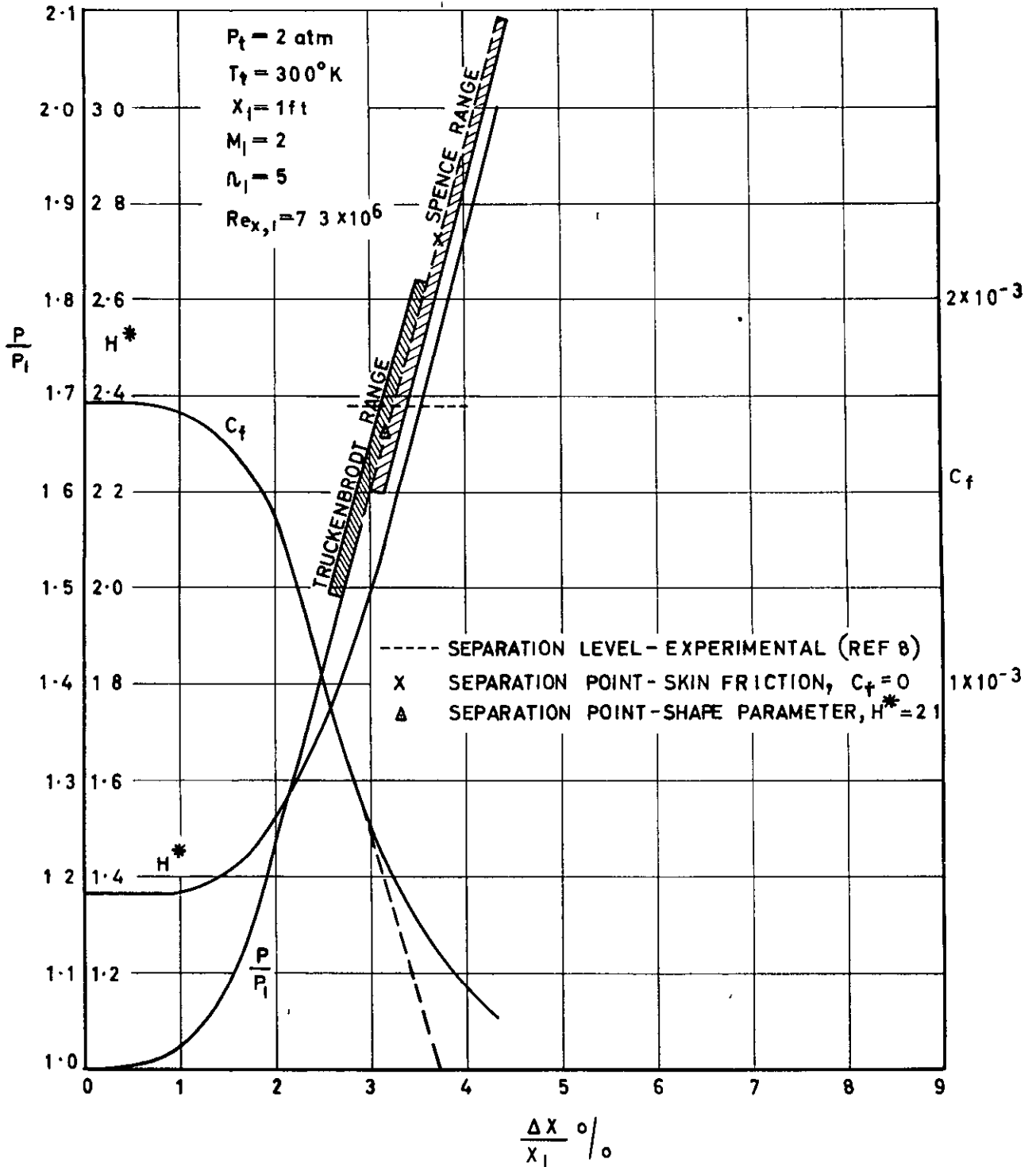
EFFECT OF LENGTH AND REYNOLDS NUMBER.

FIG. 9



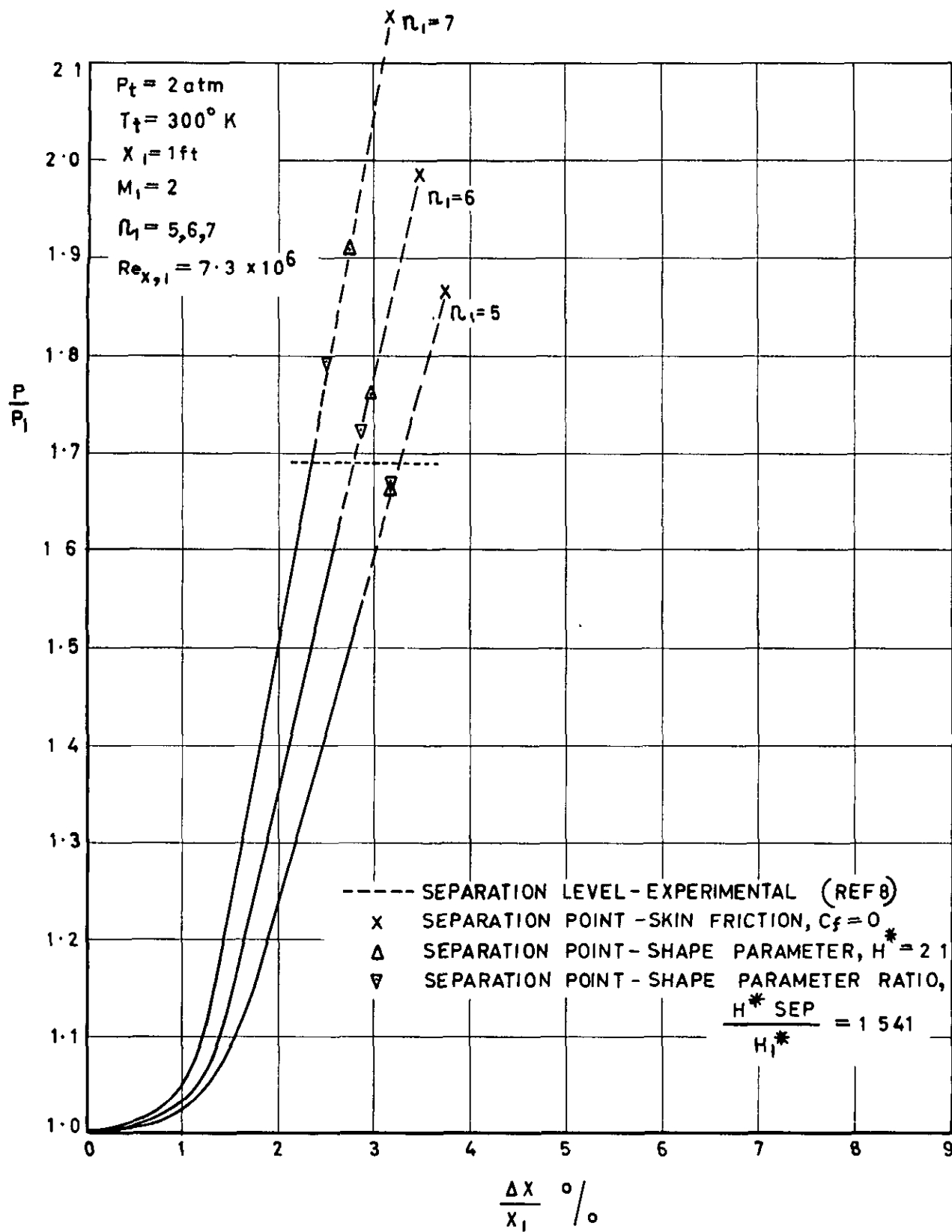
MACH NUMBER 1.5 RESULTS.

FIG. 10



SEPARATION PREDICTION METHODS.

FIG. 11



MACH NUMBER 2 RESULTS.

A.R.C. C.P. 967
November, 1965
Herd, R.J.

THE DISTRIBUTION OF A WALL PRESSURE RISE
IN A TURBULENT BOUNDARY LAYER

An expression is derived for the wall pressure gradient in attached flow with both compressible and incompressible turbulent boundary layers. From this gradient, the pressure distribution may be determined by an integration process, and it is seen that the agreement with experiment is encouraging. Of the various potential applications of this technique, separation is here considered.

A.R.C. C.P.967
November, 1965
Herd, R.J.

THE DISTRIBUTION OF A WALL PRESSURE RISE
IN A TURBULENT BOUNDARY LAYER

An expression is derived for the wall pressure gradient in attached flow with both compressible and incompressible turbulent boundary layers. From this gradient, the pressure distribution may be determined by an integration process, and it is seen that the agreement with experiment is encouraging. Of the various potential applications of this technique, separation is here considered.

A.R.C. C.P.967
November, 1965
Herd, R.J.

THE DISTRIBUTION OF A WALL PRESSURE RISE
IN A TURBULENT BOUNDARY LAYER

An expression is derived for the wall pressure gradient in attached flow with both compressible and incompressible turbulent boundary layers. From this gradient, the pressure distribution may be determined by an integration process, and it is seen that the agreement with experiment is encouraging. Of the various potential applications of this technique, separation is here considered.

© *Crown copyright 1967*

Printed and published by
HER MAJESTY'S STATIONERY OFFICE

To be purchased from
49 High Holborn, London WC 1
423 Oxford Street, London W.1
13A Castle Street, Edinburgh 2
109 St Mary Street, Cardiff CF1 1JW
Brazenose Street, Manchester 2
50 Fairfax Street, Bristol 1
258/259 Broad Street, Birmingham 1
7-11 Linenhall Street, Belfast BT2 8AY
or through any bookseller

Printed in England